ISSN 0036-0295, Russian Metallurgy (Metally), Vol. 2022, No. 1, pp. 6–12. © Pleiades Publishing, Ltd., 2022.
Russian Text © The Author(s), 2022, published in Metally, 2022, No. 1, pp. 8–14.

Effect of the Addition of 0.5 wt % Zinc on the Microstructure and Properties of an Mg–2.3 wt % Y–0.7 wt % Zr–2.0 wt % Nd Alloy

A. S. Anishchenko[a], *, A. V. Koltygin[a], **, and V. E. Bazhenov[a], ***

[a] *National University of Science and Technology MISiS, Moscow, Russia*

**e-mail: anishchenko94@gmail.com*

***e-mail: misistlp@mail.ru*

****e-mail: v.e.bagenov@gmail.com*

Received August 27, 2021; revised September 20, 2021; accepted October 11, 2021

Abstract—The effect of zinc on the freezing range, phase composition, and mechanical properties of a high-temperature Mg–Nd–Y–Zn–Zr alloy (ML19) is considered. The ML19 alloy containing 0.5 wt % Zn and an analogous alloy free of zinc are compared. Zinc is found to weakly affect the aging time that allows the peak hardness to be reached. The considered zinc content weakly changes the phase composition of the alloy and its freezing range. The hardness, the ultimate tensile strength, and the yield strength also are almost unchanged when 0.5 wt % Zn is added. Zinc positively affects the elongation at fracture of the aged alloy: it increases it by one and a half time. Thus, 0.5% zinc is an efficient addition for the ML19 alloy.

Keywords: magnesium cast alloys, high-temperature alloys, zinc addition, ML19 alloy, Mg–Nd–Y–Zr alloys, Thermo-Calc software

DOI: 10.1134/S0036029522010025

INTRODUCTION

Magnesium alloys exhibit enhanced mechanical properties and adequate creep resistance at a high temperature and are widely used in the aircraft and aerospace industries [1–4]. Usually, these alloys are based on the Mg–REM–Zr system [5, 6]. The application of Mg–REM–Zr-based alloys ensures high strength characteristics at room temperature. Moreover, owing to adequate creep resistance of these alloys at high temperatures, parts made from them can operate at temperatures up to 300°C [7–9].

To increase the mechanical properties and creep resistance of magnesium alloys at high temperatures, rare-earth metals (REMs), such as neodymium, yttrium, and gadolinium are used; they are taken in different proportions [8]. In the case of widespread alloys, the REM content is 8–15 wt %.[1] As examples of such alloys, WE43 and WE54 alloys can be noted [9–12]. In Russia, an Mg–Y–Nd–Zr-based ML19 alloy is the most widely used. The REM contents in it are substantially lower than those in analogous alloys, such as WE43 and WE54. In contrast to these alloys, the ML19 alloy contains up to 0.6% zinc as the required alloying addition [13]. The usefulness of zinc as the alloying component is confirmed by the fact that, along with the traditional neodymium and 1.2% gadolinium additions, the zinc content in a relatively new Electon 21 magnesium alloy is up to 0.5%. The alloy can be used at temperatures up to 200°C for a long time and up to 250°C under short-time loadings, and, despite the lower total REM content, its mechanical properties remain similar to those of WE43 and WE54 alloys, which have a similar combination of alloying elements and are free of zinc [14–16]. Thus, currently, cast magnesium alloys containing REMs and zirconium as the main alloying elements are used. In this case, the zinc content in an alloy can be low or it can be free of zinc; this is explained by the ambiguous effect of small zinc additions on the properties of cast magnesium alloys. In the present study, the effect of the 0.5% Zn addition on the structure and properties of a cast Mg–2.3% Y–0.7% Zr–2.0% Nd alloy is considered.

EXPERIMENTAL

The following raw materials were used: magnesium (99.9% Mg) produced in the Solikamsk Magnesium Works (Russia); zinc (99.98% Zn); Mg–15% Zr master alloy fabricated in the Solikamsk Experimental Metallurgical Plant (Russia); magnesium alloy ML19 containing 2.2% Y, 2.36% Nd, 0.27% Zn, and 0.5% Zr, which was fabricated in the Solikamsk Experimental Metallurgical Plant (Russia); and Mg–20% Nd and Mg–20% Y master alloys produced by OOO PK Metagran (Moscow, Russia). Melting was performed in a resistance furnace in an (Ar + SF_6) protective atmosphere using steel crucibles. After adding the master alloy and heating to 750°C, the melt was held

[1] Hereafter, the element contents are given in wt %, unless otherwise stated.

Table 1. Magnesium-based alloy compositions (%)

Alloy	Y	Zr	Nd	Zn
ML19	2.3	0.6	2.0	0.5
ML19wZn	2.3	0.7	2.0	–
ML19 (State Standard 2856–79)	1.4–2.2	0.4–1.0	1.6–2.3	0.1–0.6

for 10 min and, after that, was purged with argon. After 10 min holding and slag removal, the melt at a temperature of 750°C was cast in a graphite mold. The ingots were used to prepare samples for metallographic observations, hardness measurements, and tensile tests.

The chemical composition of the prepared samples was determined by energy dispersive X-ray spectroscopy (EDS); no less than three measurements were carried out on an area of 1 × 1 mm in size for each sample. The microstructure of the alloys and the element contents in phases were studied by scanning electron microscopy (SEM) using a Vega 3SBH scanning electron microscope (Tescan, Czech republic) equipped with an energy dispersive microanalyzer (Oxford, UK).

The Brinell hardness was measured at a load of 62.5 kgf (~613 N) using a NEMESIS 9001 universal tester (Innovatest, Netherlands) and a ball of 2.5 mm in diameter; the holding time under loading was 30 s.

The mechanical properties were determined by tensile tests using an Instron 5569 (USA) universal testing machine.

The electrical conductivity was determined with a VE-27NC/4-5 contact-free eddy current conductivity meter (Sigma, Russia); the limits of effective range are 5–37 MS/m.

Vertical sections of the phase diagrams, phase composition of alloys, and their solidification in terms of a Scheil–Gulliver model were calculated using the Thermo-Calc 2016a software and the TCMG4 thermodynamic database (Magnesium alloys database version 4).

All tests were performed using cast and heat-treated alloys. Heat treatment (HT) was performed in accordance with the following regime: 16-h holding at 525°C + water quenching + aging at 205°C for 21 h. In the course of aging, the hardness and electrical conductivity of the samples were determined every three hours.

RESULTS AND DISCUSSION

Table 1 gives the chemical compositions of the prepared alloys. The ML19 alloy was prepared from a zinc-free ML19wZn alloy via the addition of zinc in the melt. The microstructures of ML19 and ML19wZn cast alloys were studied (Fig. 1). The as-cast microstructure of the ML19wZn alloy (Fig. 1a) consists of a magnesium-based solid solution (α-Mg) and, probably, the $Mg_{41}(Nd,Y)_5$ intermetallic phase, which forms at the boundaries of α-Mg dendrites during a eutectic reaction. The microstructure of the ML19 alloy (Fig. 1b) also consists of α-Mg dendrites and intermetallic phase formed at their boundaries. In this case, the dendrite cell size in the ML19 alloy is slightly smaller than that in the analogous ML19wZn alloy (18.69 ± 1.39 and 17.21 ± 0.92 μm, respectively). However, the decrease is so insignificant that we can state that the 0.5% Zn addition does not affect the dendrite size in the alloys under study.

Figure 2 shows vertical sections of the multicomponent Mg–Y–Zr–Nd and Mg–Y–Zr–Nd–Zn phase

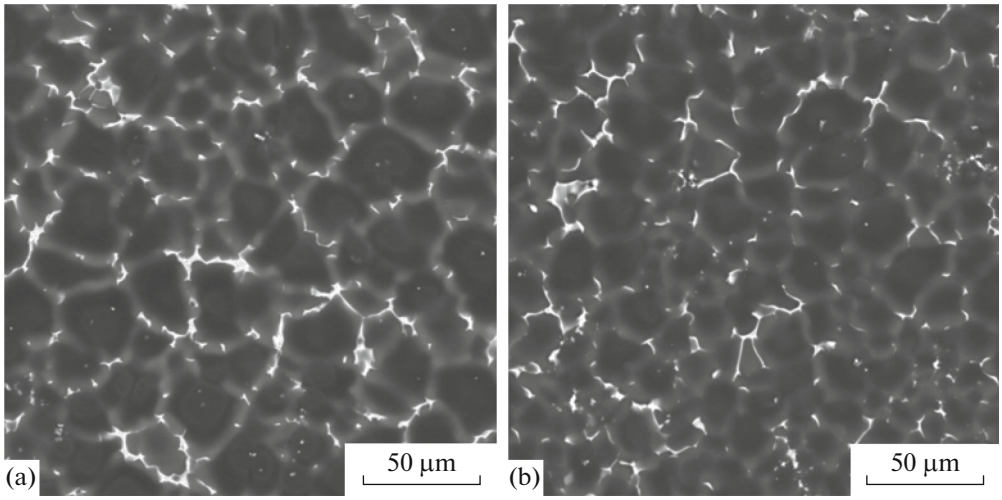

Fig. 1. Microstructure of as-cast alloys (a) ML19wZn and (b) ML19.

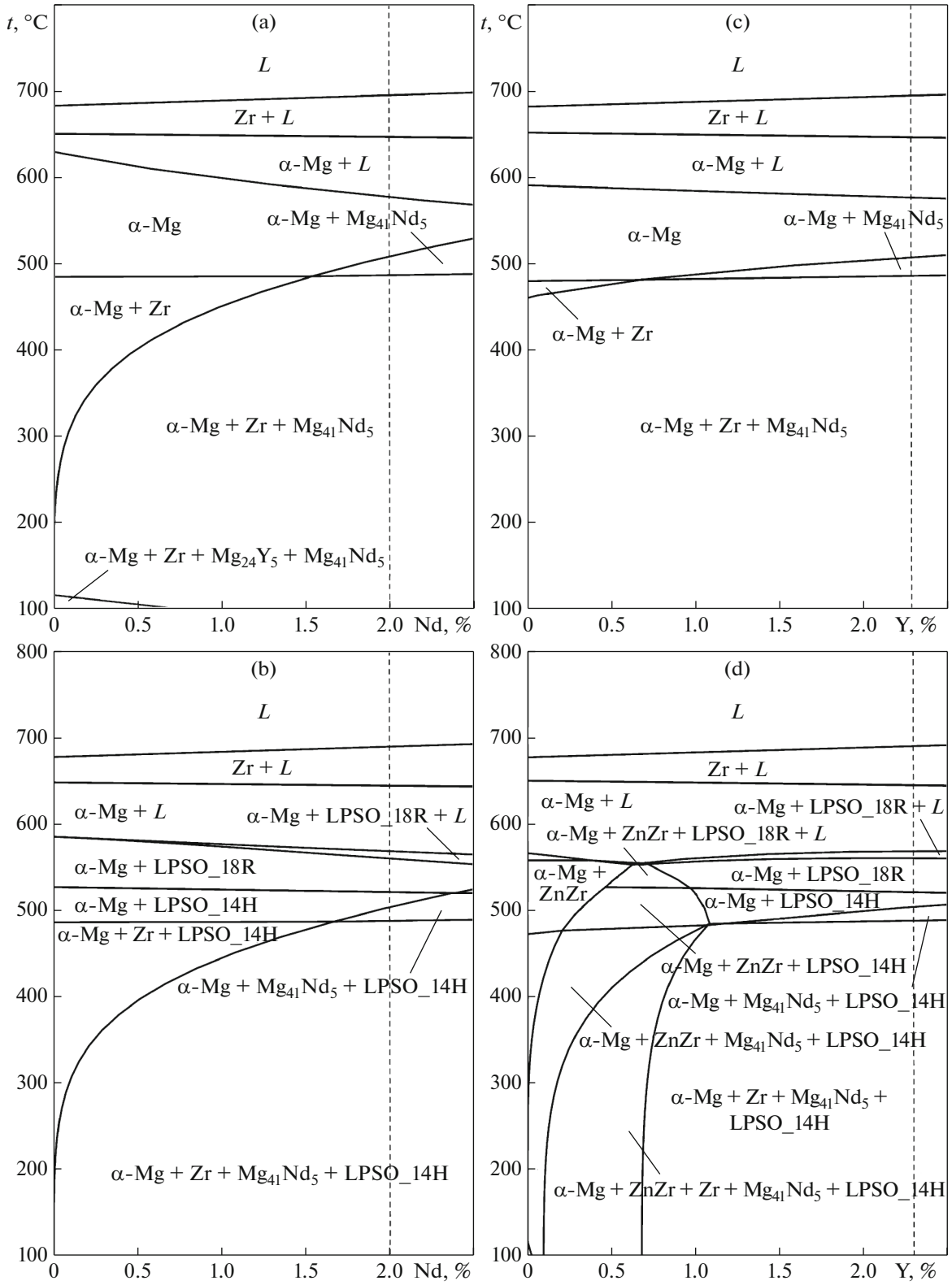

Fig. 2. Vertical sections of the phase diagrams: (a) Mg–2.3% Y–0.6% Zr–(0–2.5)% Nd, (b) Mg–2.3% Y–0.6% Zr–0.5% Zn–(0–2.5)% Nd, and (c) Mg–0.7% Zr–2.0% Nd–(0–2.5)% Y, (d) Mg–0.7% Zr–2.0% Nd–0.5% Zn–(0–2.5)% Y. Dotted lines correspond to the alloying element contents in the alloys under study; _18R and _14H are structural polytypes of the LPSO phase.

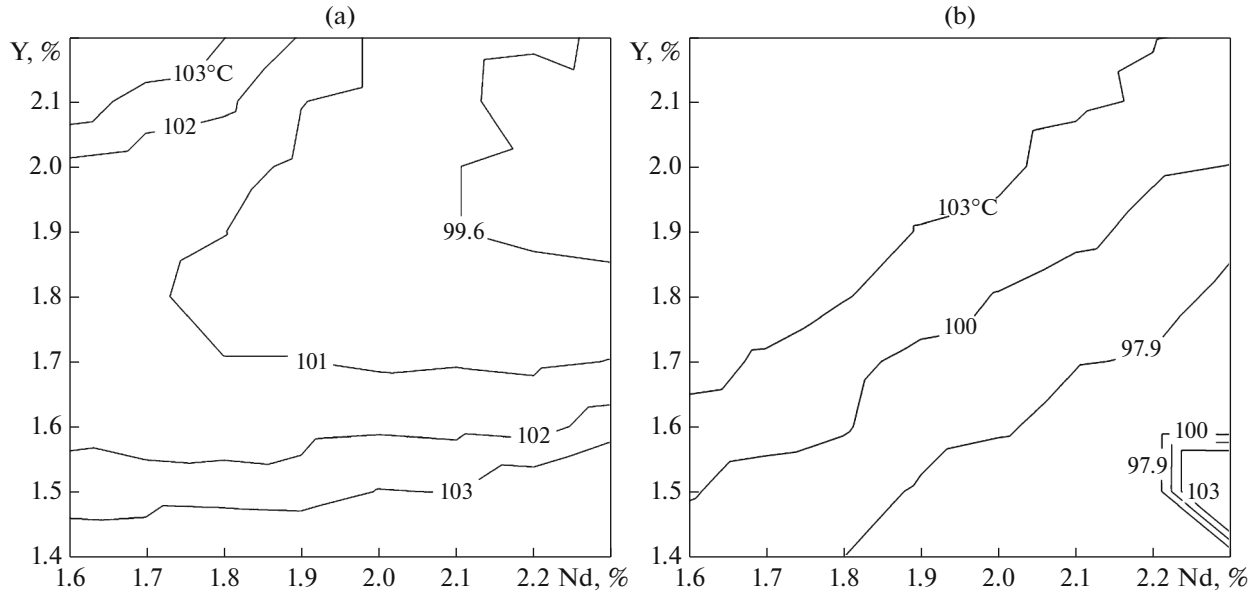

Fig. 3. Non-equilibrium solidification range in (a) Zn-containing and (b) Zn-free ML19 alloys vs. the REM content. Contours correspond to the freezing range.

diagrams that correspond to the composition region of the alloys under study. The composition of the alloys (see Table 1) is shown with dotted lines in Fig. 2. The solidification of the alloys free of zinc (Figs. 2a, 2c) is seen to begin with the precipitation of zirconium crystals at the liquidus temperature, which slightly increases as the neodymium and yttrium contents in the alloys increase, and to end in the precipitation of the α-Mg. An increase in the neodymium content in the alloy leads to a decrease in the equilibrium solidus temperature, whereas the yttrium content weakly affects the solidus temperature. The added zinc content does not affect radically the solidification pathway (Figs. 2b, 2d); in this case, solidification ends in the precipitation of the α-Mg and a small amount of LPSO phase. However, the LPSO phase was not found in the alloy microstructures (Fig. 1).

Thus, based on the analysis of the microstructures, we can state that zinc weakly affects the solidification behavior of the alloys under study. Nevertheless, an analysis of the vertical sections of the multicomponent phase diagrams indicates the possibility of the formation of a structure containing the LPSO phase, which was not found by EDS. The LPSO-phase content is likely to be too low to be detected by the methods used in the present study, since information about the existence of the LPSO phase in the ML19 alloy is available [17].

Figure 3 shows the effect of the yttrium and neodymium contents on the non-equilibrium solidification range of the alloys; the dependences are based on the calculations performed with the Thermo-Calc software using the Scheil–Gulliver nonequilibrium solidification model. This effect is of high importance, since the widening of the freezing range of an alloy usually negatively affects its casting properties. In particular, the alloys characterized by long freezing range exhibit a low fluidity and usually are prone to form isolated porosity in castings [18]. In the composition region with the yttrium and neodymium contents close to those in the ML19 alloy, it is possible to observe that these elements very weakly affect the alloy freezing range. The shortest freezing range is observed in the case of the maximum yttrium and neodymium contents. At comparable REM contents, the alloy containing 0.5% Zn and the alloy free of zinc exhibit almost the same non-equilibrium freezing ranges (in the case of the Zn-containing alloy, the range is 3–7°C longer). Since the zinc addition weakly affects the freezing range of the alloys under study, their castability should not be worsened with adding zinc.

Figure 4 shows the variations of the hardness *HB* of experimental alloys as the time of artificial aging (τ_{ag}) at 205°C increases; the hardness of the as-cast alloys is also given. After quenching, the hardness of the ML19 alloy is seen to be lower than that of the ML19wZn alloy. However, after 15-h aging, the hardnesses of the alloys under study become almost the same because of solid-solution depletion. Holding at the aging temperature for more than 15 h leads to a decrease in the hardness because of over-aging of the alloys under study.

Figure 5 shows the dependences of the electrical conductivities of the alloys on the aging conditions during HT. The zinc addition is seen to decrease the electrical conductivities of the alloys in both the as-cast and heat-treated states. This is related to the dis-

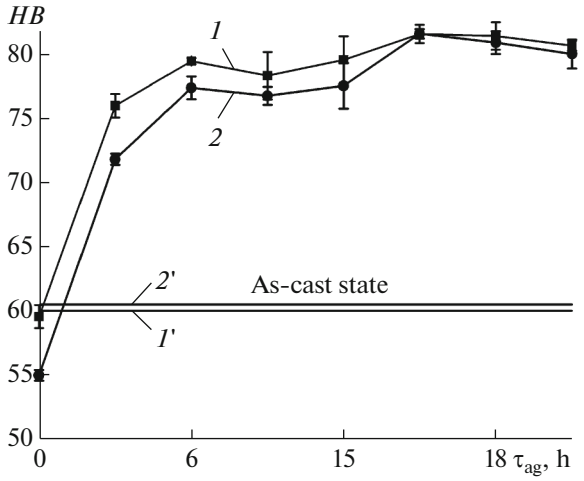

Fig. 4. Variations of the hardness *HB* of the alloys (*1*) ML19wZn and (*2*) ML19 in the course of aging after isothermal holding at 525°C for 16 h and water quenching. Horizontal lines *1*' and *2*' indicate the hardness of as-cast alloys *1* and *2*, respectively.

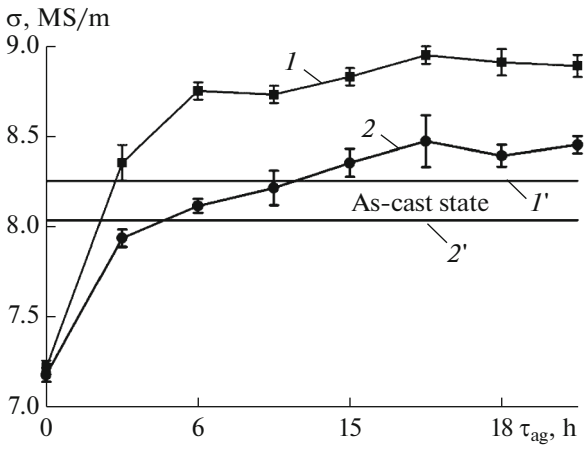

Fig. 5. Variations of the electrical conductivity of the alloys (*1*) ML19wZn and (*2*) ML19 in the course of aging after isothermal holding at 525°C for 16 h and water quenching. Horizontal lines *1*' and *2*' indicate the electrical conductivities of as-cast alloys *1* and *2*, respectively.

solution of zinc in the α-Mg. The peak electrical conductivities of the alloys are reached after 15-h aging. These data correlate with the variations of the hardness during HT. Thus, we can state that the maximum aging time of these alloys should not exceed 15 h, and the alloying with 0.5% zinc does not affect the aging time.

To perform tensile tests, samples were subjected to HT in accordance with regime T6, which includes isothermal holding at 525°C for 16 h, subsequent quenching in hot water, and aging at 205°C for 15 h. As was shown above, these conditions should ensure the peak strengthening of the alloys.

Figure 6 shows the microstructures of the ML19wZn and ML19 alloys subjected to HT. Note that the HT leads to a decrease in the fraction of REM-containing intermetallics in the alloy structure; in this case, zirconium phase particles are not dissolved. No radical differences in the structures of the ML19wZn and ML19 alloys is observed; in this case, EDS allows us to detect zinc in both the α-Mg and the intermetallic phases in the ML19 alloy.

According to the results of mechanical tests of the ML19 and ML19wZn alloys, the ultimate tensile strength of these alloys is σ_u = 245–255 MPa and the yield strength is $\sigma_{0.2}$ ~ 150 MPa. The elongation at fracture δ of the ML19wZn alloy is less than that of the ML19 alloy by almost 2%. The ultimate tensile strength and the yield strength of this alloy also slightly decrease. The effect of zinc on the mechanical proper-

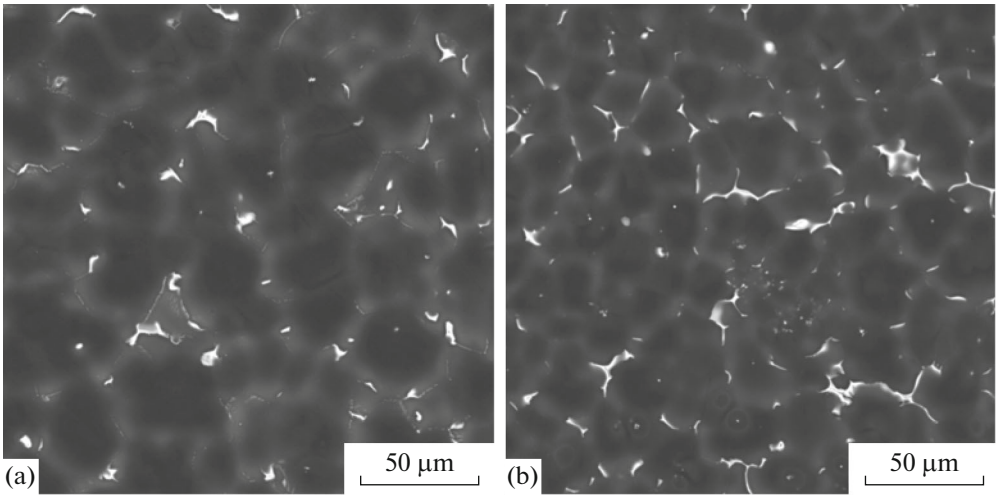

Fig. 6. Microstructure of heat-treated alloys (a) ML19wZn and (b) ML19.

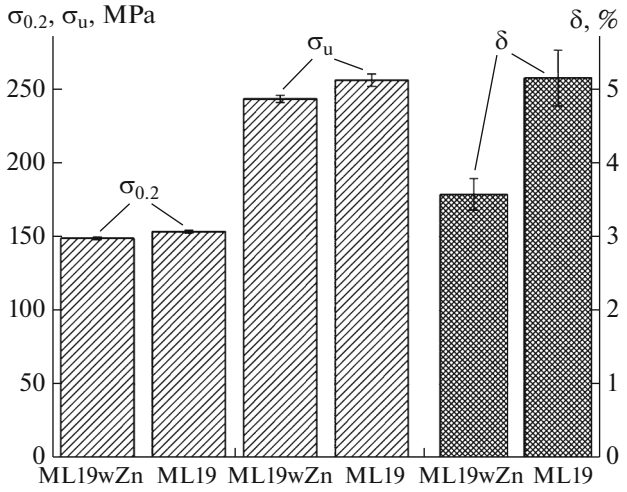

Fig. 7. Mechanical properties of the alloys ML19 and ML19wZn after heat treatment in regime T6 (16-h holding at 525°C + quenching in hot water + 15-h aging at 205°C).

ties of the alloy is explained primarily by the strengthening of the α-Mg. This effect results from precipitation of strengthening zinc-containing particles, in particular, Zn_2Zr_3. Aggregates of such particles in the microstructure are observed usually near primarily zirconium particles [19]. The increase in the elongation at fracture of the alloys after adding zinc can be related to decreasing the brittleness along grain boundaries because of entering zinc in the precipitated REM- and yttrium-containing intermetallics.

CONCLUSIONS

(1) The addition of 0.5% zinc to an Mg–Nd–Y–Zr alloy weakly affected its microstructure, phase composition, solidification pathway and freezing range.

(2) The effect of zinc on the aging rate of the alloys under study was found to be weak. The peak values of the hardness and electrical conductivity of the zinc-containing and zinc-free alloys were reached after 15-h aging. In this case, the hardness was almost the same (80 *HB*).

(3) The 0.5 wt % zinc addition to the alloy leads to an increase in its elongation at fracture from 3.5 to 5.2%; in this case, the ultimate tensile strength and the yield strength of the alloys remained almost unchanged. Thus, the addition of 0.5 wt % Zn to an Mg–Nd–Y–Zr alloy was found to positively affect its mechanical properties, in particular, its plasticity (elongation at fracture).

CONFLICT OF INTEREST

The authors declare that they have no conflicts of interest.

REFERENCES

1. *ASM Specialty Handbook: Magnesium and Magnesium Alloys*, Ed. by M. M. Avedesian and H. Baker (ASM International, 1999).
2. B. L. Mordike and T. Ebert, "Magnesium: properties—applications—potential," Mater. Sci. Eng. A **302** (1), 37–45 (2001).
3. A. Nayeb-Hashemi, *Phase Diagrams of Binary Magnesium Alloys* (ASM International Metals Park, Ohio, 1988).
4. E. Piyush, R. Raghu, M. S. Rakesh, and S. G. Sriram, "Magnesium alloy casting technology for automotive applications—a review," IRJET **4**, 675–681 (2017).
5. J. Li, R. Chen, Y. Ma, and W. Ke, "Effect of Zr modification on solidification behavior and mechanical properties of Mg–Y–RE (WE54) alloy," J. Magnes. Alloys **1** (4), 346–351 (2013).
6. Z. Yang, J. P. Li, J. X. Zhang, G. W. Lorimer, and J. A. M. Robson, "Review on research and development of magnesium alloys," Acta Metallurgica **21** (5), 313–328 (2009).
7. W. Unsworth, "Meeting the high temperature aerospace challenge," Light Metal Age **44** (7, 8), 15–18 (1986).
8. Z. Trojanova, T. Donič, P. Lukač, P. Palček, M. Chalupova, E. Tillova, and R. Bašt'ovanský, "Tensile and fracture properties of an Mg–RE–Zn alloy at elevated temperatures," J. Rare Earths **32** (6), 564–572 (2014).
9. I. Polmear, D. St. John, J. F. Nie, and M. Qian, *Light Alloys: Metallurgy of the Light Metals* (Butterworth-Heinemann, 2017).
10. Z. Xu, M. Weyland, and J. F. Nie, "On the strain accommodation of β_1 precipitates in magnesium alloy WE54," Acta Mater. **75**, 122–133 (2014).
11. Y. H. Kang, D. Wu, R. S. Chen, and E. H. Han, "Microstructures and mechanical properties of the age hardened Mg–4.2 Y–2.5 Nd–1Gd–0.6 Zr (WE43) mi-

croalloyed with Zn," J. Magnes. Alloys **2** (2), 109–115 (2014).

12. Y. Yang, X. Xiong, J. Chen, X. Peng, D. Chen, and F. Pan, "Research advances in magnesium and magnesium alloys worldwide in 2020," J. Magnes. Alloys **9** (3), 705–747 (2021).

13. A. V. Koltygin, V. E. Bazhenov, N. V. Letyagin, and V. D. Belov, "The Influence of Composition and Heat Treatment on the Phase Composition and Mechanical Properties of ML19 Magnesium Alloy," Russ. J. Non-Ferr. Met. **59**, 32–41 (2018).

14. A. Kielbus, "Microstructure and properties of Elektron 21 magnesium alloy," J. Magnes. Alloys: Des. Process. Prop. **4**, 281–296 (2011).

15. A. Kiełbus, "Corrosion resistance of Elektron 21 magnesium alloy," J. Achiev. Mater. Manufact. Eng. **22** (1), 29–32 (2007).

16. A. Kiełbus, "TEM investigations of Electron 21 magnesium alloy," Solid State Phenom. **130**, 175–180 (2007).

17. M. V. Anikina, E. F. Volkova, I. V. Mostyaev, and N. V. Trofimov, "Study of the structure and phase composition of a serial magnesium alloy ML19 in the cast and heat-treated states," in *Metal Science and Modern Developments of Casting, Deformation, and Anticorrosion Protection Technologies of Light Alloys: Materials of All-Russian Scientific and Technical Conference, Moscow, 2019* (Izd. VIAM, Moscow, 2019), pp. 7–20.

18. M. V. Pikunov, *Metal Melting, Alloy Crystallization, Ingot Solidification* (Izd. MISiS, Moscow, 2005).

19. S. Abd El Majid, G. Atiya, M. Bamberger, and A. Katsman, "Nucleation and growth of metastable phases in Mg–Nd, Mg–Gd and Mg–Gd–Nd based alloys," in *Proceedings of Symposium Magnesium Technology 2014, San Diego* (2014), p. 179.

Translated by N. Kolchugina